Tumor promoter TPA activates Wnt/β-catenin signaling in a casein kinase 1-dependent manner

Zijie Su[a,b,1], Jiaxing Song[a,b,1], Zhongyuan Wang[a,1], Liang Zhou[a], Yuqing Xia[a], Shubin Yu[a], Qi Sun[a], Shan-Shan Liu[a], Liang Zhao[a], Shiyue Li[a], Lei Wei[b], Dennis A. Carson[a,c,2], and Desheng Lu[a,2]

[a]Guangdong Key Laboratory for Genome Stability & Disease Prevention, Carson International Cancer Center, Department of Pharmacology, Shenzhen University Health Science Center, Shenzhen, 518060 Guangdong, China; [b]Department of Pathology and Pathophysiology, School of Basic Medical Sciences, Wuhan University, Wuhan, 430071 Hubei, China; and [c]Moores Cancer Center, University of California, San Diego, La Jolla, CA 92093

The tumor promoter 12-O-tetra-decanoylphorbol-13-acetate (TPA) has been defined by its ability to promote tumorigenesis on carcinogen-initiated mouse skin. Activation of Wnt/β-catenin signaling has a decisive role in mouse skin carcinogenesis, but it remains unclear how TPA activates Wnt/β-catenin signaling in mouse skin carcinogenesis. Here, we found that TPA could enhance Wnt/β-catenin signaling in a casein kinase 1 (CK1) ε/δ-dependent manner. TPA stabilized CK1ε and enhanced its kinase activity. TPA further induced the phosphorylation of LRP6 at Thr1479 and Ser1490 and the formation of a CK1ε–LRP6–axin1 complex, leading to an increase in cytosolic β-catenin. Moreover, TPA increased the association of β-catenin with TCF4E in a CK1ε/δ-dependent way, resulting in the activation of Wnt target genes. Consistently, treatment with a selective CK1ε/δ inhibitor SR3029 suppressed TPA-induced skin tumor formation in vivo, probably through blocking Wnt/β-catenin signaling. Taken together, our study has identified a pathway by which TPA activates Wnt/β-catenin signaling.

TPA | CK1 | LRP6 | Wnt/β-catenin signaling | two-stage skin chemical carcinogenesis

The Wnt/β-catenin signaling pathway plays a crucial role in embryonic development, stem cell self-renewal, and tumorigenesis (1–4). In the absence of Wnt proteins, β-catenin is constantly degraded by a destruction complex containing the scaffolding protein axin, the adenomatosis polyposis coli (APC) protein, the enzyme glycogen synthase kinase-3β (GSK3β), and casein kinase 1 (CK1). The Wnt/β-catenin signaling cascade is initiated when the secreted Wnt proteins bind to the low-density lipoprotein receptor-related protein 5/6 (LRP5/6) and a member of the Frizzled (Fzd) family (2, 5). Subsequently, CK1 is activated and phosphorylates Dishevelled (Dvl) (6). Receptor complexes further cluster on platforms of oligomerized Dvl, leading to the formation of LRP6 signalosomes (7, 8). Receptor clustering triggers phosphorylation of LRP6 by multiple CK1 members following priming by GSK3β and recruits the axin complex to signalosomes (8). As a consequence, phosphorylation of β-catenin is inhibited. Unphosphorylated β-catenin accumulates in the cytoplasm and translocates into the nucleus, where it binds transcription factors of the T-cell factor/lymphoid enhancing factor (TCF/LEF) family and recruits the transcriptional Kat3 coactivators p300 and/or CREB-binding protein, finally leading to the expression of Wnt target genes (9, 10).

The CK1 family of serine/threonine kinases consists of six human isoforms (α, δ, ε, γ1, γ2, and γ3). All members share a highly conserved amino-terminal kinase domain. Among them, CK1ε and CK1δ display the highest consensus, with a 98% sequence identity in their kinase domain and 53% identity in their C-terminal regulatory domain (11, 12). CK1 members phosphorylate several key regulatory molecules in the Wnt/β-catenin signaling pathway and exert dual functions, acting either as inhibitors or activators of the pathway (13, 14). In the β-catenin destruction complex, CK1α phosphorylates β-catenin at Ser45 and primes β-catenin for further phosphorylation by GSK3β and subsequent degradation (10). Moreover, CK1ε and CK1δ are

able to phosphorylate APC in cooperation with GSK3β, resulting in an increase in affinity of APC to β-catenin and its ability to down-regulate β-catenin (6). Upon Wnt stimulation, CK1ε activity is rapidly up-regulated and phosphorylates Dvl at multiple sites (15, 16), which is required for LRP6 signalosome formation and LRP6 phosphorylation at Thr1479 and Ser1490 (8). CK1ε can also phosphorylate TCF3, thereby increasing its binding to β-catenin (17).

TPA (12-O-tetra-decanoylphorbol-13-acetate) is generally known for its tumor-promoting activity in two-stage skin chemical carcinogenesis (18). It specifically induces clonal expansion of initiated cells carrying activated ras oncogenes (19), resulting in tumor development. Although protein kinase C (PKC) family members have been identified as the main targets of TPA (20), their role in tumor promotion remains controversial (21). So far, clinical trials using PKC inhibitors for the treatment of cancer have been ineffective (21, 22). A meta-analysis of several clinical trials for non-small-cell lung carcinomas revealed worsened patient outcome when PKC inhibitors were combined with chemotherapy compared with chemotherapy alone (23). The results from other clinical trials also showed that targeting PKC in cancer is not an effective approach to therapy (24, 25). Furthermore, Antal et al. (21) recently observed that cancer-associated mutations in PKC are generally loss-of-function,

Significance

The phorbol ester 12-O-tetra-decanoylphorbol-13-acetate (TPA) is a well-known tumor promoter in two-stage mouse skin carcinogenesis, but the exact mechanism by which TPA promotes tumorigenesis remains elusive. This study discovered that TPA could stabilize CK1ε, enhance its kinase activity, and induce phosphorylation of LRP6, resulting in the formation of CK1ε–LRP6–axin1 complex, which may bypass the requirement of Wnt–Fzd–Dvl complex. TPA also increased the interaction between β-catenin and TCF4E in a CK1ε/δ-dependent way, and finally led to activation of the Wnt/β-catenin pathway. Our findings reveal a pathway by which TPA activates the Wnt/β-catenin signaling cascade. This pathway may represent a common mechanism for the tumor-promoting activity of some carcinogenic agents.

suggesting that PKC isozymes generally function as tumor suppressors. However, the PKC family is not the sole receptor for the phorbol esters. Several non-PKC proteins have been identified as new phorbol ester receptors, including protein kinase D (26), diacylglycerol kinases (27, 28), guanine nucleotide exchange factors for small GTPases (RasGRPs) (29), GTPase-activating proteins (chimaerin Rac-GAPs) (30), and components of the synaptic vesicle fusion protein complex (Munc-13 isoforms) (31). The discovery of these novel phorbol ester receptors raises the hypothesis that the tumor-promoting effect of various phorbol esters may proceed through PKC-independent pathways.

In two-stage skin chemical carcinogenesis, a single topical application of a carcinogen DMBA (7,12-dimethylbenz[a]anthracene) on the mouse skin, followed by repeated applications of TPA, results in the formation of benign skin papillomas, of which some progress into invasive squamous cell carcinomas (18, 32, 33). H-ras mutation is a hallmark of DMBA/TPA-induced skin papillomas (34). Mutations of the H-ras oncogene activate several downstream pathways, including Ras/Raf/ MAPK/ERK and PI3K/Akt (35, 36). Activation of PKCs by TPA may also lead to enhanced Ras/Raf-1/MAP kinase signaling (37). Additionally, TPA can induce activation of AP-1 and NF-κB transcription factors in mouse skin through effects on ERK, c-Jun NH2-terminal kinase, Akt, and p38 MAPK (38).

The Wnt/β-catenin signaling pathway plays a decisive role in skin tumorigenesis (39). Transgenic mice expressing a constitutively activated version of β-catenin develop skin tumors resembling pilomatricomas (40). Keratinocyte-specific knockout of the Ctnnb1 gene (encoding β-catenin) prevents DMBA/TPA-induced tumorigenesis in mouse skin (41, 42). The ablation of β-catenin function in established DMBA/TPA-induced tumors leads to their complete regression (43). Moreover, DMBA/TPA-induced tumors showed cytoplasmic and nuclear accumulation of β-catenin and up-regulation of Wnt target genes (c-myc and c-jun). TCF4 was found to be a major effector in Wnt/β-catenin signaling in mouse skin carcinogenesis (44). Apparently, TPA-induced tumorigenesis is associated with activation of Wnt/β-catenin signaling. However, it is not yet clear how TPA activates Wnt/β-catenin signaling in the two-stage carcinogenesis model. In the present study, we found that TPA stabilized CK1ε and enhanced its kinase activity. TPA further induced the phosphorylation of LRP6 and the formation of a CK1ε–LRP6–axin1 complex, thus bypassing the requirement for a Wnt–Fzd–Dvl complex. Furthermore, TPA treatment promoted the association of β-catenin with TCF4E in a CK1ε/δ-dependent manner. Importantly, a specific CK1ε/δ inhibitor SR3029 blocked DMBA/TPA-induced skin tumorigenesis in vivo, probably through inhibition of Wnt/β-catenin signaling.

Results

TPA Enhances Wnt/β-Catenin Signaling Activated by CK1ε. The calcium ionophore ionomycin exerts antagonistic activity on the Wnt/β-catenin pathway by increasing intracellular calcium levels (45). The elevation of intracellular calcium levels may activate PKC. We compared the effects of ionomycin and the PKC activator TPA on Wnt/β-catenin signaling. The SuperTopFlash reporter system was used to determine the activation of Wnt/β-catenin signaling in response to ionomycin and TPA. The SuperTopFlash reporter was transfected into HEK293T cells along with Wnt1, Wnt1/LRP6, Wnt3/LRP6, Dvl2, and CK1ε expression plasmids, respectively. As expected, ionomycin and TPA inhibited Wnt signaling activated by Wnt1 (Fig. 1 *A* and *D*), Wnt1/LRP6 (*SI Appendix*, Fig. S1 *A* and *D*), Wnt3/LRP6 (*SI Appendix*, Fig. S1 *B* and *E*), and Dvl2 (*SI Appendix*, Fig. S1 *C* and *F*) in a dose-dependent manner, respectively. Moreover, the increased SuperTopFlash activity induced by Wnt3A-conditioned medium (Wnt3A-CM) was dose-dependently blocked by either ionomycin or TPA (Fig. 1 *B* and *E*). Surprisingly, ionomycin and
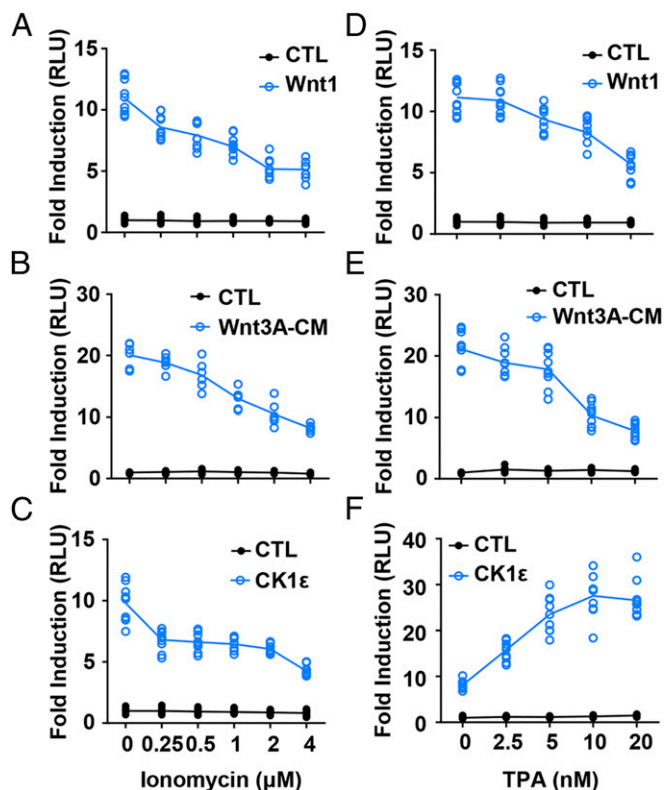

Fig. 1. TPA enhances Wnt/β-catenin signaling activated by CK1. (*A*) A SuperTopFlash reporter gene was transfected into HEK293T cells together with empty vector or Wnt1 expression plasmid. The transfected cells were treated with vehicle or the indicated concentrations of ionomycin before being assayed for luciferase activity. (*B*) The SuperTopFlash reporter gene was transfected into HEK293T cells, after which the cells were treated with control or Wnt3A-CM. The cells were treated with vehicle or increasing concentrations of ionomycin as indicated. (*C*) HEK293T cells were transfected with the SuperTopFlash reporter gene and empty vector or an expression plasmid for CK1ε. The cells were incubated with vehicle or increasing concentrations of ionomycin as indicated. (*D*) Similar to *A* except that the indicated concentrations of TPA were used. (*E*) Similar to *B* except that the indicated concentrations of TPA were used. (*F*) Similar to *C* except that the indicated concentrations of TPA were used. The luciferase values were normalized to β-gal activities. Results are expressed as fold induction compared with empty vector control. The results were the average from at least three independent experiments done by duplicates, n ≥ 6.

TPA differentially regulated the transcriptional activity of the SuperTopFlash reporter in HEK293T cells transfected with a CK1ε expression plasmid. TPA dose-dependently enhanced CK1ε-mediated reporter transcription, while ionomycin repressed this effect (Fig. 1 *C* and *F*). To test whether TPA has any effect on the expression of Wnt target genes in a CK1ε-dependent manner, the CK1ε expression plasmid was transfected in HEK293T cells. Cells were then incubated overnight with 10 nM TPA. Quantitative PCR was performed to detect the mRNA expression of Wnt target genes DKK1, Fra-1, and Fosb. TPA significantly increased mRNA expression levels of Wnt target genes DKK1, Fra-1, and Fosb in a CK1ε-dependent way (*SI Appendix*, Fig. S2A). These results suggest that TPA may have a positive regulatory effect on CK1ε-mediated Wnt signaling via a calcium/PKC-independent mechanism.

To examine the effect of TPA on other signaling pathways, transfection assays were performed using an NFAT reporter (NFAT-Luc) and a Hippo reporter (8 × GTIIC-Luc). The expression plasmids encoding NFATc1 and YAP were used to activate the NFAT and Hippo signaling pathways in HEK293T

CELL BIOLOGY

cells, respectively. As shown in *SI Appendix*, Fig. S2 *B and C*, TPA had no effect on the luciferase activity of NFAT-Luc and 8 × GTIIC-Luc (*SI Appendix*, Fig. S2 *B and C*).

Effects of Other Phorbol Esters and PKC Modulators on CK1ε-Mediated Wnt Signaling. We examined the effects of other phorbol esters on CK1ε-mediated Wnt signaling. Similar to TPA (*SI Appendix*, Fig. S3A), phorbol 12, 13-didecanoate (PDD) and phorbol 12, 13-dibutyrate (PDBu) increased the luciferase activity of a SuperTopFlash reporter in HEK293T cells overexpressing CK1ε in a dose-dependent fashion (*SI Appendix*, Fig. S3 *B and C*). In contrast, a non-tumor-promoting phorbol ester, 4α-PDD, had no effect on CK1ε-mediated Wnt signaling (*SI Appendix*, Fig. S3D).

Some PKC modulators, including three PKC activators (DOG, DHI, and OAG) and two PKC inhibitors (NPC15437 dihydrochloride and Gö 6976) were used to explore the role of PKC in CK1-mediated activation of Wnt signaling in response to TPA. Unlike TPA, none of the PKC activators increased SuperTopFlash reporter activity in cells overexpressing CK1ε (*SI Appendix*, Fig. S4 *A–C*), while two PKC inhibitors showed little inhibitory effect on reporter gene transcription mediated by CK1ε (*SI Appendix*, Fig. S4 *D and E*). These results

indicate that PKC may not be involved in CK1ε-mediated activation of Wnt signaling in response to TPA.

CK1ε and CK1δ Are Major Effectors of TPA-Induced Wnt Signaling. To determine which member of the CK1 family plays a more important role in TPA-induced Wnt signaling, HEK293T cells were transfected with a SuperTopFlash reporter plasmid together with CK1α, CK1γ, CK1ε, and CK1δ expression plasmids, respectively. Treatment with TPA dramatically increased transcriptional activity mediated by either CK1ε or CK1δ in a dose-dependent manner, whereas TPA had much weaker effect on CK1α-mediated transcription (Fig. 2A). TPA treatment had no effect on CK1γ-mediated transcription. The immunoblotting results with an anti-Flag antibody showed that TPA treatment dose-dependently increased the expression of CK1ε and CK1δ, while TPA had negligible effects on the expression of CK1α and CK1γ (Fig. 2B). These results indicate that CK1ε and CK1δ are major effectors of TPA-induced Wnt signaling and TPA may regulate the protein expression of CK1ε and CK1δ.

To validate the specific role of CK1ε/δ in TPA-induced Wnt signaling, dominant negative mutants of CK1ε/δ and specific CK1 inhibitors were used to test the effect of TPA on CK1ε/δ-mediated
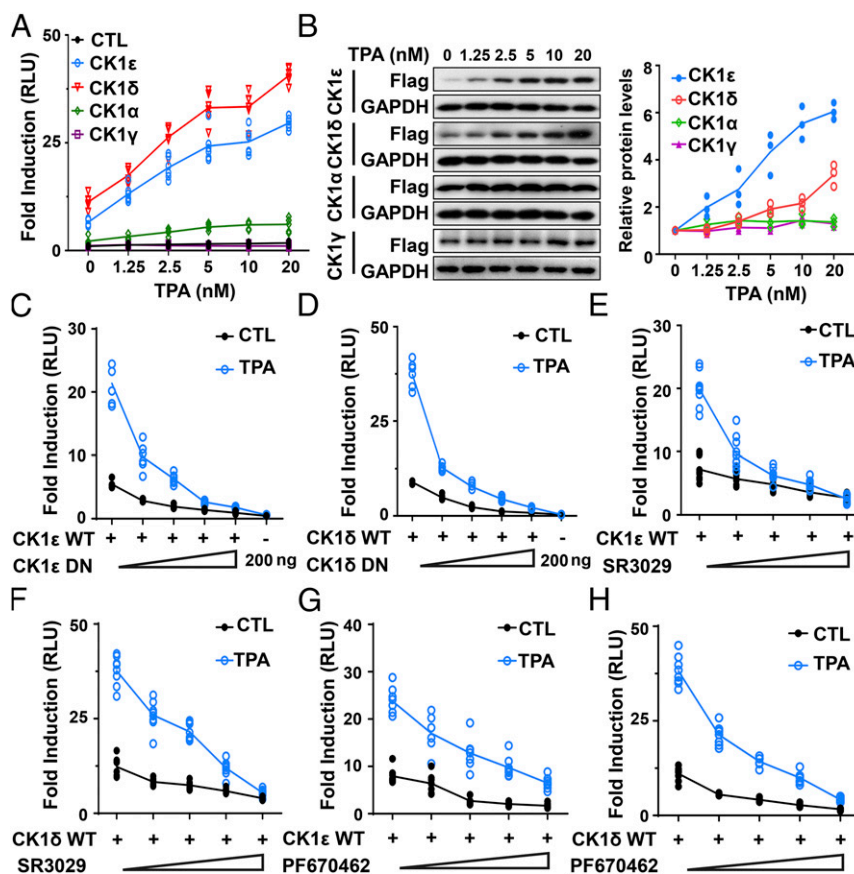
Fig. 2. CK1ε and CK1δ are major effectors of TPA-induced Wnt signaling. (A) HEK293T cells were transfected with the SuperTopFlash reporter gene together with empty vector or expression plasmids encoding CK1α, CK1γ, CK1ε, and CK1δ, respectively. The transfected cells were treated with vehicle or increasing concentrations of TPA as indicated. (B) Protein expression of CK1 isoforms and GAPDH were detected by immunoblotting using anti-Flag and anti-GAPDH antibodies. Data shown were representative of three independent experiments. The protein levels of CK1 isoforms were quantitated by densitometry and normalized to GAPDH. Quantitated results were displayed at the right. (C) The SuperTopFlash reporter gene was transfected into HEK293T cells together with 50 ng wild-type CK1ε, either alone or in combination with increasing amounts of dominant negative construct (0, 25, 50, 100, and 200 ng) and incubated with or without 10 nM TPA. (D) Similar to C except that wild-type CK1δ and its dominant negative construct were used. (E) HEK293T cells cotransfected with the SuperTopFlash reporter gene and CK1ε expression vector were incubated with or without 10 nM TPA in the presence of increasing concentrations of SR3029 (0, 15, 30, 60, and 120 nM). (F) Similar to E except that CK1δ expression vector was used. (G) Similar to E except that increasing concentrations of PF670462 (0, 0.25, 0.5, 1, and 2 μM) were used. (H) Similar to F except that increasing concentrations of PF670462 (0, 0.25, 0.5, 1, and 2 μM) were used. The luciferase activities were measured and values were normalized to β-gal activity. Results are expressed as fold induction compared with empty vector control. The results were the average from at least three independent experiments done by duplicates ($n \geq 6$).

transcription. Increasing concentrations of dominant negative mutants of CK1ε (Fig. 2C) or CK1δ (Fig. 2D) blocked wild-type CK1ε/δ-mediated transcriptional activity of a SuperTopFlash reporter in response to TPA. Furthermore, specific CK1ε/δ inhibitors SR3029 and PF670462 markedly inhibited TPA-induced transcriptional activation in the presence of CK1ε or CK1δ (Fig. 2 E–H).

TPA Regulates the Expression and Subcellular Localization of CK1ε and CK1δ. We next examined the effect of TPA on expression levels of the CK1ε and CK1δ proteins in HEK293T and melanoma

UACC903 cells. Western blot analyses showed that TPA augmented expression of endogenous CK1ε and CK1δ in a time- and dose-dependent manner in both cell lines (Fig. 3 A and B). We then determined if TPA affects the half-life of CK1ε and CK1δ proteins. Protein translation was inhibited by cycloheximide (CHX). The results showed that treatment with CHX reduced the levels of endogenous CK1ε and CK1δ in a time-dependent manner in HEK293T cells, and addition of TPA increased the half-life of CK1ε and CK1δ proteins (Fig. 3C). Treatment with the proteasome inhibitor MG132 also enhanced TPA-induced accumulation of CK1ε and CK1δ in both cell lines (Fig. 3D), suggesting that the
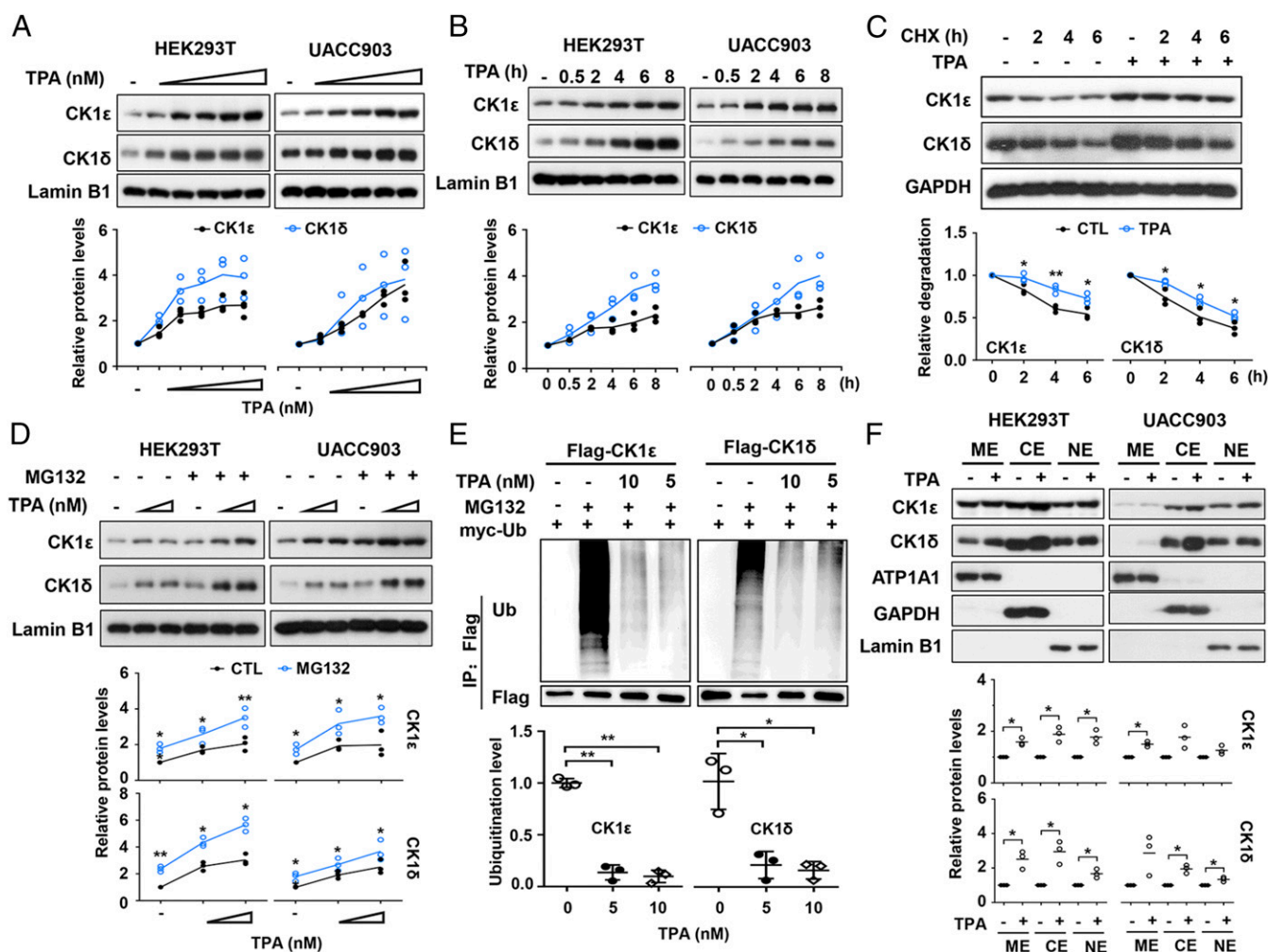
Fig. 3. TPA regulates the expression and subcellular localization of CK1ε and CK1δ. (A) HEK293T and UACC903 cells were incubated with TPA at increasing concentrations (0, 2, 10, 50, 100, and 200 nM). The whole-cell extracts were analyzed by immunoblotting using the indicated antibodies. The protein levels of CK1ε and CK1δ were quantitated by densitometry and normalized to Lamin B1. Quantitated results are displayed (*Bottom*). (B) HEK293T and UACC903 cells were incubated with 10 nM TPA for the indicated time period. The expression of CK1ε and CK1δ proteins were assessed by immunoblotting. The protein levels of CK1ε and CK1δ were quantitated by densitometry and normalized to Lamin B1. Quantitated results are displayed (*Bottom*). (C) HEK293T cells were pretreated with 10 nM TPA for 2 h before 100 μg/mL CHX was added. The cells were harvested after CHX treatment for the indicated times (0, 2, 4, and 6 h) followed by immunoblotting. The protein levels of CK1ε and CK1δ were quantitated by densitometry and normalized to GAPDH. Quantitated results were plotted against indicated time periods to dynamic changes and are displayed (*Bottom*). *$P < 0.05$, **$P < 0.01$ versus vehicle control (Student's t test, $n = 3$). (D) HEK293T and UACC903 cells were incubated with increasing concentrations of TPA (0, 100, and 200 nM) for 6 h and then were treated with 10 μM MG132 for 1 h. The cells were harvested and the levels of CK1ε and CK1δ proteins were detected by immunoblotting. The protein levels of CK1ε and CK1δ were quantitated by densitometry and normalized to Lamin B1. Quantitated results are displayed (*Bottom*). (E) HEK293T cells cotransfected with Flag-CK1ε/δ and myc-ubiquitin (Ub) expression vectors were incubated with or without the indicated concentrations of TPA for 18 h before treatment with 10 μM MG132 for 6 h. Cell lysates were subjected to immunoprecipitation using anti-Flag M2 Sepharose (Sigma) followed by Western blot using specific antibodies as indicated. Ubiquitination of CK1ε and CK1δ protein was quantitated by densitometry from three independent experiments and normalized to Flag levels. Quantitated results were plotted against indicated concentrations of TPA to ubiquitination levels. *$P < 0.05$, **$P < 0.01$ versus the corresponding vehicle control (Student's t test, $n = 3$). (F) HEK293T cells and UACC903 cells were treated with 10 nM TPA for 6 h, and subcellular fractions were isolated from the whole-cell extracts by Subcellular Protein Fractionation Kit according to the manufacturer's protocol (Thermo). The protein levels were detected by immunoblotting using specific antibodies as indicated. Data shown are representative from three independent experiments. Protein levels were quantified by densitometry and normalized to the corresponding loading control. CE, cytoplasmic extract; ME, membrane extract; NE, nuclear extract. *$P < 0.05$ versus the corresponding vehicle control (Student's t test, $n = 3$).

increased levels of CK1ε and CK1δ may be due to decreased degradation. In contrast, TPA had negligible effects on the half-life of dominant negative CK1ε in HEK293T cells transfected with dominant negative CK1ε (*SI Appendix*, Fig. S5*A*).

To test the effect of TPA on the ubiquitination of CK1ε and CK1δ, Flag-tagged CK1ε/δ and myc-tagged ubiquitin expression vectors were cotransfected into HEK293T cells. Cells were incubated with 5 nM and 10 nM TPA for 18 h before treatment with 10 μM MG132 as indicated in Fig. 3*E*. The cell lysates were subjected to immunoprecipitation using anti-Flag antibody followed by separation on SDS/PAGE and immunoblotting analysis with anti-ubiquitin and anti-Flag antibodies. As shown in Fig. 3*E*, TPA significantly decreased the ubiquitination of CK1ε and

CK1δ (Fig. 3*E*). However, TPA did not affect the ubiquitination of dominant negative CK1ε/δ (*SI Appendix*, Fig. S5*B*). These results suggest that TPA negatively mediates the ubiquitination of CK1ε and CK1δ.

To determine whether TPA can influence subcellular localization of CK1ε and CK1δ, we examined the subcellular distribution of endogenous CK1ε and CK1δ after TPA treatment. HEK293T and UACC903 cells were incubated with 10 nM TPA for 6 h, and cell fractions were subjected to Western blot analysis. The protein levels of subcellular fractions were quantitated by densitometry. The results showed that TPA induced an increase in the protein levels of CK1ε and CK1δ in the membrane, nuclear, and cytoplasmic fractions in HEK293T and UACC903 cells,
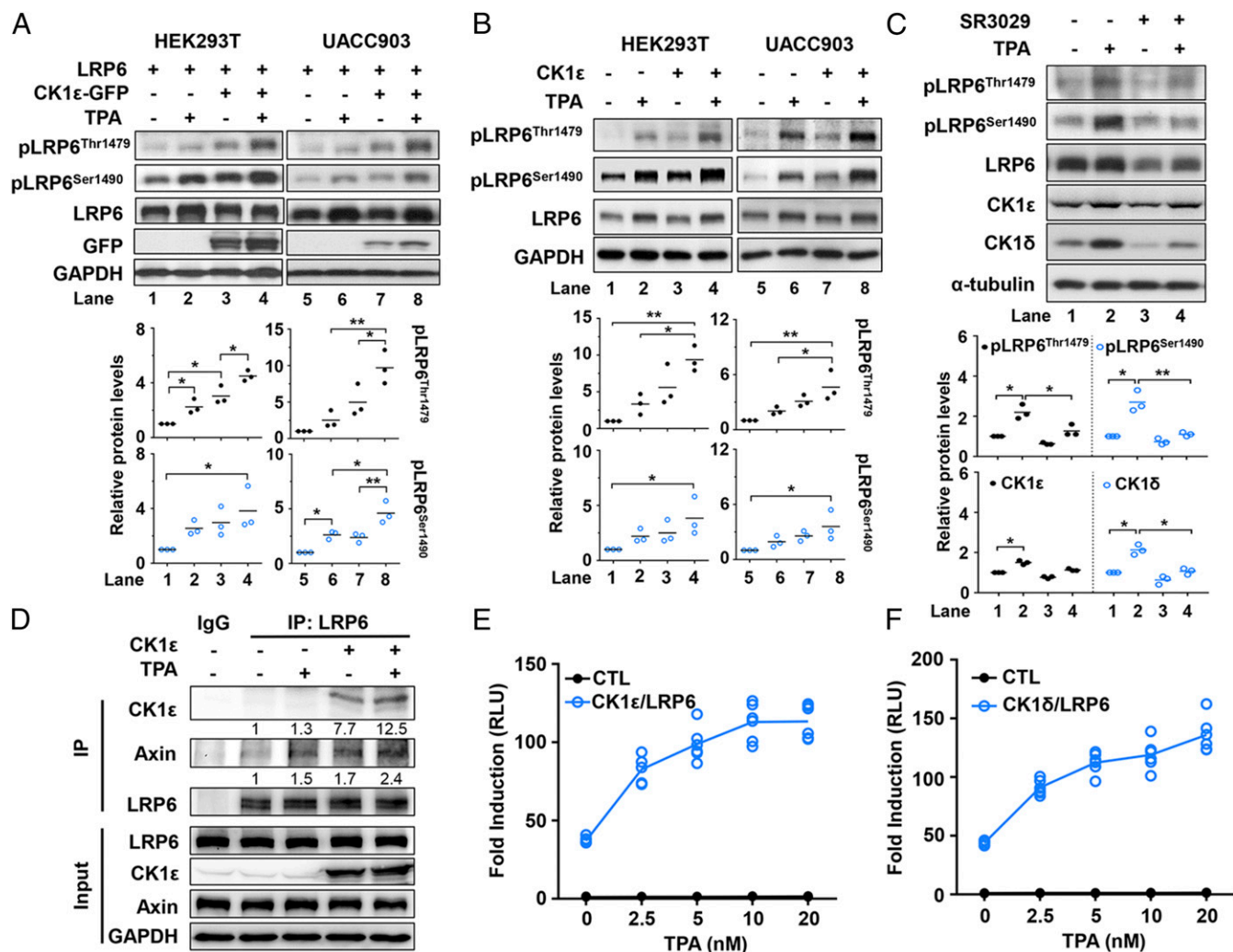
Fig. 4. TPA induces the phosphorylation of LRP6 and the formation of a CK1ε–LRP6–axin1 complex. (*A*) HEK293T and UACC903 cells cotransfected with CK1ε-GFP and LRP6 expression vectors were treated with 10 nM TPA for 6 h. Cell lysates were analyzed by immunoblotting using specific antibodies as indicated. The levels of phosphorylated Thr1479 and Ser1490 forms of LRP6 were quantitated by densitometry and normalized to GAPDH levels. *$P < 0.05$, **$P < 0.01$ versus vehicle control (one-way ANOVA, $n = 3$). Quantitated results are displayed (*Bottom*). (*B*) HEK293T and UACC903 cells transfected with a CK1ε expression plasmid were treated with or without 10 nM TPA for 6 h. The levels of phosphorylated Thr1479 and Ser1490 forms of LRP6 were quantitated by densitometry and normalized to GAPDH levels. *$P < 0.05$, **$P < 0.01$ versus vehicle control (one-way ANOVA, $n = 3$). (*C*) UACC903 cells were incubated with 10 nM TPA in the presence or absence of 60 nM SR3029 for 6 h. The levels of phosphorylated Thr1479 and Ser1490 forms of LRP6 were quantitated by densitometry and normalized to GAPDH levels. *$P < 0.05$, **$P < 0.01$ versus vehicle control (one-way ANOVA, $n = 3$). (*D*) HEK293T cells were transfected with or without a Flag-CK1ε expression plasmid in the absence or presence of 10 nM TPA for 6 h. Cell lysates were subjected to immunoprecipitation with ant-LRP6 antibody followed by immunoblotting analysis using the indicated antibodies. Protein levels were quatified by densitometry and normalized to LRP6 levels. (*E*) The SuperTopFlash reporter gene was transfected into HEK293T cells together with expression vectors encoding LRP6 and CK1ε. Transfected cells were incubated with increasing concentrations of TPA as indicated. (*F*) Similar to *E* except that expression vectors for LRP6 and CK1δ were used. Luciferase activity was measured and presented as fold induction compared with empty vector control. Data were collected from three independent experiments done by duplicates ($n = 6$).

while TPA-induced increase did not occur evenly in different fractions (Fig. 3*F*).

TPA Decreases the Level of Phosphorylated Dvl. Wnt-induced phosphorylation of Dvl is an essential step in Wnt/β-catenin signaling. Dvl proteins have been shown to be CK1ε/δ substrates in vivo. Upon Wnt stimulation, CK1ε/δ phosphorylates Dvl at distinct Ser/Thr residues (6, 16). We examined the effect of treatment with TPA on Dvl phosphorylation in HEK293T and UACC903 cells. TPA treatment decreased the levels of phosphorylated Dvl2, which was visualized as a slower-migrating band on SDS/PAGE, in both cell lines (*SI Appendix*, Fig. S6). The TPA-induced decrease of phosphorylated Dvl2 might be attributed to its activation of calcium/PKC signaling since ionomycin also caused a similar decrease in phosphorylation of Dvl2 (*SI Appendix*, Fig. S6).

TPA Induces the Phosphorylation of LRP6 and the Formation of CK1ε–LRP6–Axin1 Complex. Considering the critical role of LRP6 phosphorylation in Wnt/β-catenin signaling, we examined the effect of CK1ε on TPA-induced phosphorylation of LRP6. HEK293T and UACC903 cells were transfected with an LRP6 expression vector in the absence or presence of an expression plasmid encoding CK1ε. As shown in Fig. 4 *A* and *B*, TPA induced the phosphorylation of endogenous and exogenous LRP6 at Thr1479 and Ser1490 in both cell lines, and stronger effects were observed in the cells transfected with the CK1ε expression vector (Fig. 4 *A* and *B*). Ser1490 of LRP6 can be phosphorylated by multiple kinases, including GSK3β, GRK5, and ERK kinases (8). A previous study showed that TPA could induce Ser1490 LRP6 phosphorylation by activating ERK (46). We postulate that the presence of CK1ε may facilitate ERK-mediated LRP6 phosphorylation. Consistently, the CK1 inhibitor SR3029 dramatically blocked TPA-mediated LRP6 phosphorylation at Thr1479 and Ser1490 in UACC903 cells (Fig. 4*C*).

To identify the downstream interacting partners of CK1ε in response to TPA, a Flag-tagged CK1ε expression vector was transfected into HEK293T cells. At 6 h after treatment with 10 nM TPA, cell lysates were isolated and immunoprecipitated with anti-LRP6 antibody. As shown in Fig. 4*D*, overexpressing CK1ε by transfection alone enhanced the complex formation of CK1ε–LRP6–axin1, and treatment with TPA potentiated the

interaction among CK1, LRP6, and axin1 (Fig. 4*D*). These results suggest that TPA induces the formation of CK1ε–LRP6–axin1 multiprotein complex.

To test the effect of TPA on Wnt signaling activated by CK1ε/LRP6 or CK1δ/LRP6, HEK293T cells were transfected with the SuperTopFlash reporter together with expression vectors encoding CK1ε/LRP6 and CK1δ/LRP6, respectively. As expected, TPA enhanced reporter transcription activated by either CK1ε/LRP6 (Fig. 4*E*) or CK1δ/LRP6 (Fig. 4*F*) in a dose-dependent fashion.

CK1ε Phosphorylates LRP6 at Thr1479 in Vitro and TPA Enhances the Kinase Activity of CK1ε. Thr1479 residue of LRP6 is a typical casein kinase target (8). Since TPA treatment increased the interaction between CK1ε and LRP6, it is reasonable to assume that CK1ε may directly phosphorylate LRP6 at Thr1479. To determine if CK1ε directly phosphorylates LRP6 at Thr1479, an in vitro kinase assay was performed. The recombinant GST-LRP6 mini fusion protein was incubated with the purified CK1ε enzyme in a reaction buffer containing 200 μM ATP. The phosphorylation of Thr1479 was determined by using the phospho-specific antibody for detection of the phosphorylated Thr1479 residue of LRP6. The results showed that the purified CK1ε directly phosphorylated Thr1479 in the GST-LRP6 mini construct (Fig. 5*B*). Treatment with TPA dose-dependently increased CK1ε kinase activity (Fig. 5*C*), while CK1ε-induced LRP6 phosphorylation at Thr1479 was strongly inhibited by a specific CK1 inhibitor, PF670462 (Fig. 5*B*). Additionally, TPA rescued the inhibitory effect of PF670462 on the kinase activity of CK1ε (Fig. 5*D*). These results indicate that Thr1479 residue of LRP6 is a CK1ε phosphorylation site and TPA could enhance the kinase activity of CK1ε.

TPA Enhances the Level of Cytosolic β-Catenin in a CK1ε/δ-Dependent Fashion. To test whether TPA affects the level of cytosolic β-catenin in a CK1ε/δ-dependent fashion, HEK293T cells were transfected with wild-type CK1ε or CK1δ and dominant negative mutant of CK1ε or CK1δ, respectively. Treatment with TPA increased cytosolic β-catenin level in the presence of either CK1ε or CK1δ in a time-dependent manner (Fig. 6*A*), while dominant negative mutants of CK1ε of CK1δ did not have discernable effects on TPA-induced cytosolic β-catenin accumulation (Fig. 6*B*).
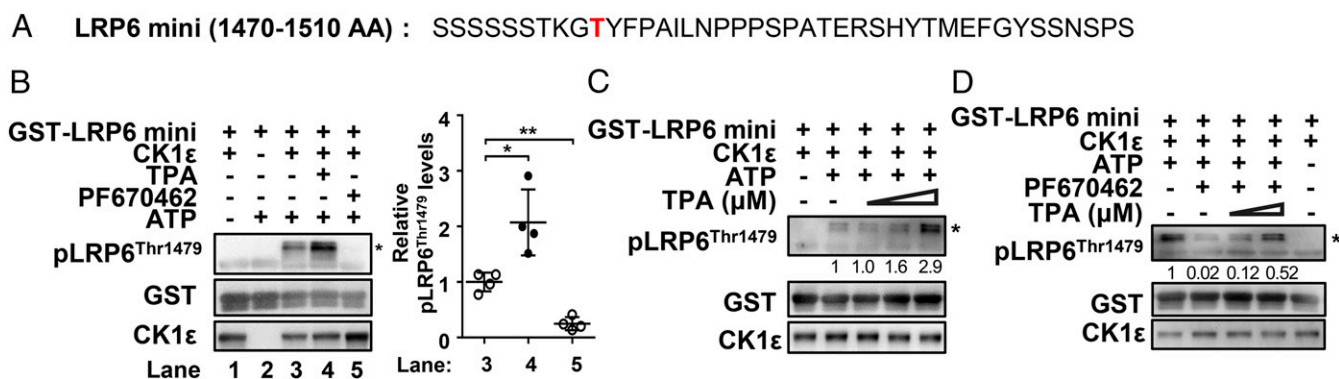
Fig. 5. CK1ε phosphorylates LRP6 at Thr1479 in vitro and TPA enhances the kinase activity of CK1ε. (*A*) The amino acid sequences of the LRP6 intracellular region (residues 1470–1510) used in this study. Thr1479 residue is indicated by red. (*B*) The recombinant CK1ε phosphorylates Thr1479 of GST-LRP6 mini fragment in vitro, and TPA enhances CK1ε kinase activity. GST-LRP6 mini fragment fusion protein was incubated with recombinant CK1ε in the presence of 200 μM ATP with or without 160 μM TPA or 2 μM PF670462 as indicated. The detection of the phosphorylation of Thr1479 was performed by immunoblotting using an anti–phospho-LRP6 (Thr1479) antibody. Thr1479 phosphorylation levels were quantitated by densitometry and normalized to GST-LRP6 mini levels. *$P < 0.05$, **$P < 0.01$ versus the corresponding vehicle control (Student's *t* test, *n* = 3). Quantitated results are displayed (*Right*). (*C*) TPA potentiated the kinase activity of CK1ε in a dose-dependent manner. The GST-LRP6 mini fusion protein was incubated with CK1ε in the absence or presence of the indicated concentrations of TPA. (*D*) TPA rescued the inhibitory effect of PF670462 on the kinase activity of CK1ε. The GST-LRP6 mini fusion protein was incubated with CK1ε in the absence or presence of 2 μM PF670462 or the indicated amounts of TPA. Thr1479 phosphorylation of GST-LRP6 mini was measured by immunoblotting using anti–phospho-LRP6 (Thr1479) antibody, indicated by p-LRP6 (Thr1479). Phosphorylation of Thr1479 is indicated by an asterisk.

CELL BIOLOGY
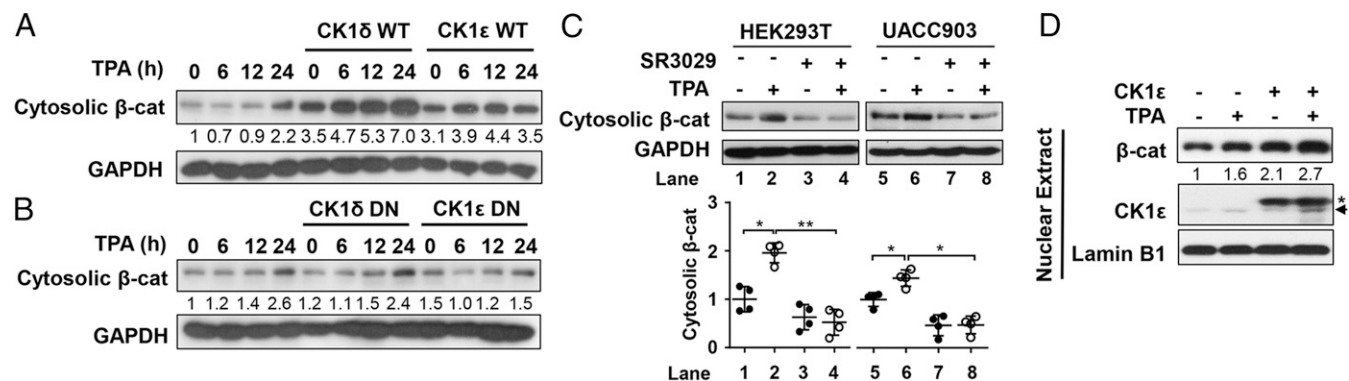
Fig. 6. TPA enhances the level of cytosolic β-catenin in a CK1ε/δ-dependent fashion. (*A*) HEK293T cells were transfected with empty vector and an expression plasmid for CK1ε or CK1δ. The cells were incubated with 10 nM TPA for the indicated time periods. Cytosolic β-catenin (β-cat) was prepared as described in *Materials and Methods*. The β-catenin expression level was detected by immunoblotting. (*B*) Similar to *A* except that dominant negative CK1ε or CK1δ expression vectors (CK1ε DN or CK1δ DN) were used. (*C*) HEK293T and UACC903 cells were incubated with 10 nM TPA in the presence or absence of 60 nM SR3029. Cytosolic β-catenin was prepared, and immunoblotting was used to detect β-catenin and GAPDH expression. The cytosolic β-catenin levels were quantified by densitometry and normalized to GAPDH. *$P < 0.05$, **$P < 0.01$ versus vehicle control (Student's *t* test, $n = 3$). Quantitated results are displayed (*Bottom*). (*D*) UACC903 cells transfected with empty vector and CK1ε expression plasmid were treated with 10 nM TPA for 6 h. Nuclear extracts were prepared using a Subcellular Protein Fractionation Kit according to the manufacturer's instructions. Fractions were analyzed by immunoblotting using the indicated antibodies. Asterisk indicates Flag-tagged CK1ε and an arrow indicates endogenous CK1ε. Protein levels were quantified by densitometry and normalized to Lamin B1.

In addition, treatment with the CK1ε/δ inhibitor SR3029 blocked TPA-induced cytosolic β-catenin accumulation in HEK293T and UACC903 cells (Fig. 6*C*). Notably, TPA increased nuclear localization of β-catenin in melanoma UACC903 cells, and a higher level of nuclear β-catenin was observed in response to TPA treatment in the cells transfected with CK1ε expression vector (Fig. 6*D*).

TPA Increases the Association of β-Catenin with TCF4E in a CK1ε/δ-Dependent Way. Given that TCF4 is a major player in Wnt/β-catenin signaling in mouse skin carcinogenesis (44), we speculated that TPA stimulation may increase β-catenin and TCF4E protein–protein interaction in a CK1ε/δ-dependent way, finally leading to the transcriptional activation of Wnt target genes. To confirm this hypothesis, HEK293T or UACC903 cells were transfected with the vectors encoding Flag-tagged versions of wild-type and dominant negative mutants of CK1ε or CK1δ, respectively. Whole-cell lysates were immunoprecipitated with anti–β-catenin antibody after treatment with TPA for 24 h. The coimmunoprecipitation results showed that TPA stimulation promotes the association of β-catenin with TCF4E in both HEK293T and UACC903 cells (*SI Appendix*, Fig. S7 *A–D*). A stronger interaction between β-catenin and TCF4E was observed in the response to TPA in cells transfected with wild-type CK1ε or CK1δ, but not in cells transfected with dominant negative mutants of CK1ε or CK1δ (*SI Appendix*, Fig. S7 *A–D*). These results indicate that CK1ε/δ may mediate TPA-induced increase in the interaction between β-catenin and TCF4E.

We next used a pDKK4-Luc reporter to evaluate whether TPA-induced transcriptional activity is associated with the interactions among β-catenin, TCF4E, and CK1ε/δ in the nucleus. The pDKK4-Luc reporter was constructed by cloning the DKK4 promoter region, which contains five putative TCF-binding sites, into a luciferase reporter vector (*SI Appendix*, Fig. S7*E*). DKK4 is a target gene of Wnt/β-catenin signaling. The activation of a pDKK4-Luc reporter gene requires the simultaneous presence of β-catenin and LEF1, while β-catenin or LEF1 alone has a moderate effect on its transcriptional activity (47). Consistently, cotransfection of a pDKK4-Luc reporter with β-catenin and TCF4E into HEK293T cells highly induced its transcriptional activity, and the presence of CK1ε further enhanced this effect (*SI Appendix*, Fig. S7*F*). TPA dramatically increased DKK4 promoter transcription mediated by β-catenin/TCF4E or β-catenin/TCF4E/CK1ε. Treatment with SR3029 abrogated the TPA-induced

effect (*SI Appendix*, Fig. S7*F*). Together, these results suggest that TPA-induced interaction among β-catenin, TCF4E, and CK1ε/δ may contribute to the transcriptional activation of Wnt target genes.

TPA Increases Expression of Wnt Target Genes. Activation of Wnt/β-catenin signaling up-regulates the transcription of many genes. CD44, cyclin D1, and DKK1 are established target genes of the Wnt/β-catenin pathway (2). Real-time PCR was employed to assess the effects of TPA on the expression of these Wnt target genes. In HEK293T and UACC903 cells, treatment with TPA (10 nM) markedly increased CD44 (*SI Appendix*, Fig. S8 *A* and *D*), cyclin D1 (*SI Appendix*, Fig. S8 *B* and *E*), and DKK1 (*SI Appendix*, Fig. S8 *C* and *F*) mRNA expression, while the CK1ε/δ inhibitor SR3029 dose-dependently abrogated the TPA-induced effects.

SR3029 Suppresses TPA-Induced Skin Tumor Formation in Vivo via Blockade of Wnt/β-Catenin Signaling in Mouse Skin Two-Stage Chemical Carcinogenesis. To determine whether blocking CK1ε/δ activity can suppress TPA-induced skin tumor formation in vivo, we tested the antitumor efficacy of SR3029, a highly selective dual CK1ε/δ inhibitor, in the DMBA/TPA skin carcinogenesis mouse model. Mice were initiated with DMBA, followed by twice weekly applications of TPA (33), along with topical application of either acetone vehicle or SR3029 immediately before the TPA application. The first papillomas appeared at 6 wk after TPA treatment, and the number of papillomas steadily increased, reaching ~18 tumors per mouse after 18 wk (Fig. 7 *A* and *B*). In the group treated with TPA-SR3029, the first tumors were observed at 8 wk, the tumors grew much more slowly than those in control group, and the average number of tumors per mouse was 4.9 after 18 wk (Fig. 7*C*). Histological analyses showed that SR3029 treatment reduced the number of Ki-67–positive cells in comparison with the controls, indicative of decreased tumor cell proliferation (Fig. 7*D*).

Immunohistochemical staining revealed that DMBA/TPA-induced tumors expressed high levels of CK1ε, CK1δ, active β-catenin, and total β-catenin, while SR3029 treatment decreased their expression (Fig. 7*D*). The immunoblot results showed that SR3029-treated tumors displayed decreased levels of LRP6, CK1ε, CK1δ, and active and total β-catenin compared with TPA-treated tumors (Fig. 7*E*). Marked reductions in the mRNA expression levels of the Wnt target genes CD44, cyclin D1, and Fosb were observed in SR3029-treated tumors (Fig. 7*F*).
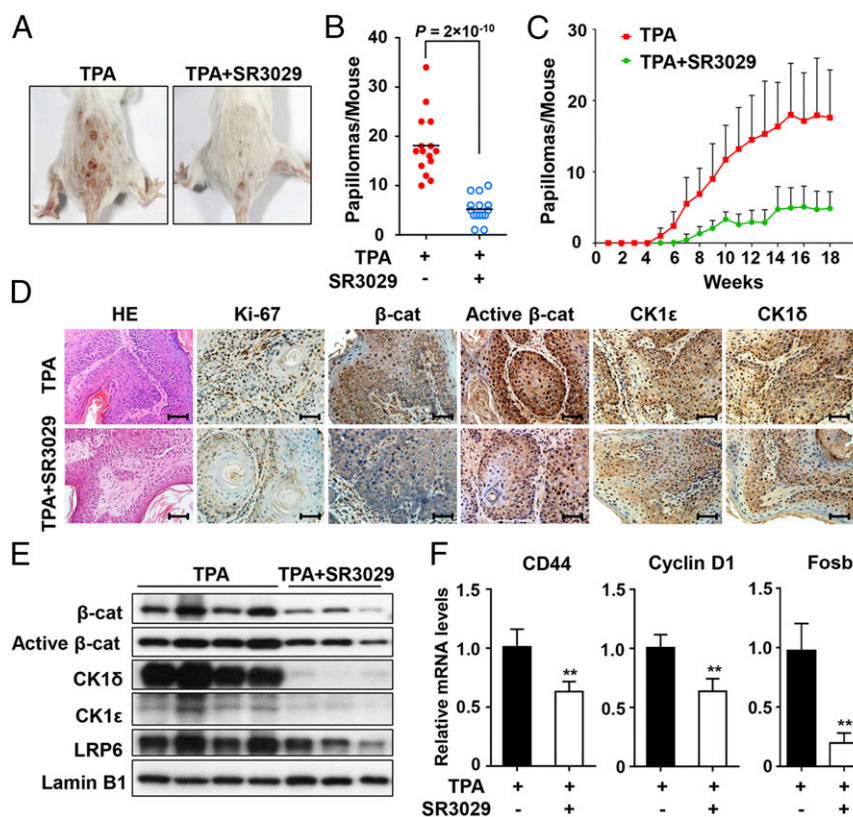
Fig. 7. SR3029 suppresses TPA-induced skin tumor formation in vivo via blockade of Wnt/β-catenin signaling in mouse skin two-stage chemical carcinogenesis. Fifteen mice per group were initiated with DMBA, followed by repetitive applications of TPA alone or together with SR3029 in acetone twice a week for 18 wk. (*A*) Images of tumors from SR3029-untreated group and SR3029-treated groups. (*B*) The average number of papillomas per mouse at the 18th wk of TPA administration in the SR3029-untreated group and the SR3029-treated group are compared (Student's *t* test, $n = 15$). (*C*) The average number of papillomas per mouse at the indicated times in SR3029-untreated group and SR3029-treated group are shown. The results are presented as mean ± SD. (*D*) Hematoxylin/eosin staining and immunohistochemistry staining using antibodies specific for Ki-67, β-catenin, active β-catenin, CK1ε, and CK1δ. (Scale bars: 100 μm.) (*E*) Expression levels of β-catenin, active β-catenin, CK1ε, CK1δ, and LRP6 in tumor samples were visualized after immunoblotting. (*F*) The mRNA expression levels of CD44, cyclin D1, and Fosb in tumor tissues were quantitated by real-time PCR. The results are shown as mean ± SD from three independent experiments (**$P < 0.01$, Student's *t* test, $n = 8$).

These results indicate that SR3029 suppressed murine skin tumorigenesis induced by DMBA/TPA, probably via blocking the Wnt/β-catenin signaling cascade.

Discussion

TPA is a well-known tumor promoter in two-stage mouse skin carcinogenesis. The Wnt/β-catenin signaling pathway has been shown to be constitutively activated in DMBA/TPA-induced skin tumors (43, 44). However, it is not clear how this pathway is activated in response to DMBA/TPA treatment. In the present study, we demonstrated that TPA could enhance Wnt/β-catenin signaling in a CK1ε/δ-dependent manner. TPA stabilized CK1 by inhibiting the ubiquitin-proteasome degradation system, enhanced its kinase activity, and induced phosphorylation of LRP6, which may trigger the formation of CK1ε–LRP6–axin1 complex, leading to an increase in the cytosolic β-catenin. Moreover, TPA could increase β-catenin and TCF4E protein-protein interaction in a CK1ε/δ-dependent way, finally resulting in the activation of Wnt target genes. Importantly, treatment with a highly selective CK1ε/δ inhibitor SR3029 suppressed TPA-induced skin tumor formation in vivo, probably through blocking Wnt/β-catenin signaling. Taken together, our results define a pathway by which TPA can activate the Wnt/β-catenin signaling cascade. This pathway may play an important role in the tumor-promoting activity of TPA in mouse skin carcinogenesis.

Binding of Wnt ligand to the Fzd receptor and coreceptor LRP6 triggers recruitment of the scaffold protein Dvl to the plasma membrane (3). Dvl promotes LRP6 aggregation and phosphorylation at Thr1479 by CK1γ (7, 48). This phosphorylation event facilitates recruitment of the negative regulator axin to the plasma membrane. Subsequently, axin-mediated β-catenin phosphorylation and degradation is inhibited, allowing accumulation of β-catenin (9). Our results imply that TPA treatment can bypass the requirement for a Wnt–Fzd–Dvl complex. TPA stabilized CK1ε, enhanced its kinase activity, and induced phosphorylation of LRP6 at Thr1479 and Ser1490. Our results provide direct evidence that the Thr1479 residue of LRP6 is a CK1ε phosphorylation site. While Ser1490 does not serve as a direct substrate for CK1, TPA could induce phosphorylation of LRP6 at Ser1490 via activation of ERK MAP kinases (8, 46). Our results suggest that the presence of CK1ε may enhance TPA-induced phosphorylation at Ser1490 by ERK. It is reasonable that TPA-induced phosphorylation of LRP6 facilitates the formation of a CK1ε–LRP6–axin complex by recruiting axin to the plasma membrane, leading to cytosolic accumulation of β-catenin.

Relatively little is known concerning the mechanisms involved in regulating the expression and activity of CK1 isoforms. The CK1δ and CK1ε isoforms are autorepressed enzymes. Their kinase activities can be regulated by inhibitory autophosphorylation at their C-terminal regions (11–13). Recently, the DEAD-box RNA helicase DDX3 was identified as a regulator

CELL BIOLOGY

of the Wnt/β-catenin signaling pathway by acting as a regulatory subunit of CK1ε in a Wnt-dependent manner (49). It binds to CK1ε, directly stimulates its kinase activity, and promotes phosphorylation of Dvl, resulting in stabilization of β-catenin. Our study demonstrated that TPA exerts multiple actions on CK1ε/δ and CK1ε/δ-mediated Wnt signaling. First, TPA induces intracellular accumulation of CK1ε and CK1δ by reducing their ubiquitination. This effect of TPA was observed when CK1ε and CK1δ were expressed at physiological or supraphysiological levels. Second, TPA enhances the kinase activity of CK1ε. Third, TPA enhances the association of CK1ε with LPR6, thus promoting LRP6 phosphorylation. Fourth, TPA can increase the interaction between β-catenin and TCF4E in a CK1ε/δ-dependent way. In addition, in vitro kinase assays showed that TPA could rescue the inhibitory effect of PF670462 on the kinase activity of CK1ε (Fig. 5D). Consistently, the CK1ε/δ inhibitor SR3029 exerts an inhibitory effect on TPA-induced cytosolic β-catenin accumulation (Fig. 6C). Moreover, TPA has been shown to block the ubiquitination of CK1ε and CK1δ (Fig. 3E). These results imply that TPA may directly interact with CK1ε/δ. However, the dominant negative forms of CK1ε/δ could not respond to TPA in the ubiquitination assay (*SI Appendix*, Fig. S5B), suggesting that the physical interaction of TPA with CK1ε/δ requires autophosphorylation of CK1ε/δ. It is very interesting to further characterize the molecular mechanism by which TPA or other phorbol esters activate Wnt signaling in a CK1ε/δ-dependent manner.

TPA effectively activates PKC by mimicking its physiologic ligand diacylglycerol (DAG) (50). PKC isozymes can be classified into three subgroups based on differences in sequence homology and biochemical properties: the Ca^{2+}- and DAG-dependent conventional PKC (cPKCα, βI, βII, and γ), the DAG-dependent novel PKC (nPKCδ, θ, ε, and η), and the Ca^{2+}- and DAG-independent atypical PKC (aPKCι and ζ) (22). It is well-documented that PKC isozymes are implicated in the regulation of the Wnt signaling pathway. Different PKC isozymes can exert opposite effects on Wnt/β-catenin signaling. PKCα and PKCδ could negatively modulate Wnt/β-catenin signaling by regulating β-catenin stability, whereas PKCε and PKCζ play important roles in the positive regulation of the Wnt/β-catenin pathway (51, 52). We tested effects of some PKC modulators on Wnt signaling in the presence or absence of CK1ε or CK1δ. Strikingly, none of three PKC activators stimulated the activation of Wnt/β-catenin signaling in cells transfected with expression vectors encoding CK1ε or CK1δ. Also, two PKC inhibitors do not influence Wnt signaling in the presence of CK1ε or CK1δ. These results suggest that PKC may not be involved in CK1-mediated activation of Wnt signaling in response to TPA.

CK1ε and CK1δ are implicated in the control of the mammalian circadian clock by phosphorylating core clock proteins (53). It is interesting to speculate that TPA may affect the circadian period via a CK1ε/δ-dependent manner. A previous study reported that TPA could advance the hamster circadian rhythms (54). In NIH 3T3 fibroblasts, TPA treatment has been shown to induce the circadian oscillation of expression of various clock and clock-related genes (55). Future studies are needed to investigate the role of CK1ε/δ in TPA-mediated circadian rhythms.

Increasing evidence has implicated CK1ε/δ as positive regulators of Wnt/β-catenin signaling (11, 13). However, the roles of CK1ε/δ in human cancer are still poorly understood. CK1ε expression has been shown to be up-regulated in adenoid cystic carcinomas of the salivary gland, in epithelial ovarian cancer, in tumors of brain, head and neck, kidney, bladder, lung, prostate, and salivary gland, and in leukemia, melanoma, and seminoma (11). Elevated protein levels of CK1δ and CK1ε were also observed in tumor cells of grade 3 ductal pancreatic carcinomas (56). Rosenberg et al. (57) recently identified CK1δ as an efficacious therapeutic target with potential for clinical relevance in a subset of breast cancers. Knockdown of CK1δ, or treatment with a highly selective CK1ε/δ inhibitor SR3029, induced apoptosis of CK1δ-expressing breast tumor cells and tumor regression in orthotopic models of triple-negative breast cancer, including patient-derived xenografts, and in HER2+ breast cancer models. A very recent study demonstrated that CK1ε/δ is a novel therapeutic target in chronic lymphocytic leukemia (CLL). The CK1ε/δ inhibitor PF-670462 significantly blocked microenvironmental interactions of CLL cells and delayed leukemia development and progression in the Eμ-TCL1 mouse model (58). In this study, CK1ε and CK1δ have been identified as distinctive intracellular targets of tumor-promoting TPA. Expression of CK1ε and CK1δ was required for TPA-induced activation of Wnt/β-catenin signaling. Importantly, a dual CK1ε/δ inhibitor SR3029 potently inhibited TPA-induced tumorigenesis by blocking Wnt/β-catenin signaling in a mouse skin cancer model. Collectively, these results indicated that CK1ε and CK1δ may be therapeutic targets for cancer drug development, especially for cancers with Wnt pathway activation.

In summary, our study identified a mechanism by which TPA activates Wnt/β-catenin signaling. TPA could stabilize CK1ε, enhance its kinase activity, and induce phosphorylation of LRP6, resulting in the formation of CK1ε–LRP6–axin1 complex, which may bypass the requirement of Wnt–Fzd–Dvl complex. TPA also enhanced the interaction between β-catenin and TCF4E in a CK1ε/δ-dependent way, and finally led to activation of the Wnt/β-catenin pathway. Our findings reveal a pathway by which phorbol esters such as TPA activate the Wnt/β-catenin signaling cascade. This pathway may represent a common mechanism for the tumor-promoting activity of some carcinogenic agents.

Materials and Methods

The cell lines and plasmids used in this study are described in *SI Appendix, Materials and Methods*. Details of in vitro kinase assay, luciferase reporter gene assay, subcellular fractionations, coimmunoprecipitation, quantitative real-time PCR analyses, two-stage skin carcinogenesis assays, histological analyses, and statistical analyses are provided in *SI Appendix, Materials and Methods*. All animal experiments were performed according to the protocols approved by the Administrative Committee on Animal Research of Shenzhen University.

1. Nusse R, Clevers H (2017) Wnt/β-catenin signaling, disease, and emerging therapeutic modalities. *Cell* 169:985–999.
2. Clevers H, Nusse R (2012) Wnt/β-catenin signaling and disease. *Cell* 149:1192–1205.
3. MacDonald BT, Tamai K, He X (2009) Wnt/β-catenin signaling: Components, mechanisms, and diseases. *Dev Cell* 17:9–26.
4. Willert K, et al. (2003) Wnt proteins are lipid-modified and can act as stem cell growth factors. *Nature* 423:448–452.
5. Huang H, He X (2008) Wnt/β-catenin signaling: New (and old) players and new insights. *Curr Opin Cell Biol* 20:119–125.
6. Klimowski LK, Garcia BA, Shabanowitz J, Hunt DF, Virshup DM (2006) Site-specific casein kinase 1ε-dependent phosphorylation of dishevelled modulates β-catenin signaling. *FEBS J* 273:4594–4602.
7. Bilic J, et al. (2007) Wnt induces LRP6 signalosomes and promotes dishevelled-dependent LRP6 phosphorylation. *Science* 316:1619–1622.
8. Niehrs C, Shen J (2010) Regulation of Lrp6 phosphorylation. *Cell Mol Life Sci* 67:2551–2562.
9. Kimelman D, Xu W (2006) β-catenin destruction complex: Insights and questions from a structural perspective. *Oncogene* 25:7482–7491.
10. Liu C, et al. (2002) Control of β-catenin phosphorylation/degradation by a dual-kinase mechanism. *Cell* 108:837–847.
11. Cozza G, Pinna LA (2016) Casein kinases as potential therapeutic targets. *Expert Opin Ther Targets* 20:319–340.
12. Cheong JK, Virshup DM (2011) Casein kinase 1: Complexity in the family. *Int J Biochem Cell Biol* 43:465–469.
13. Cruciat CM (2014) Casein kinase 1 and Wnt/β-catenin signaling. *Curr Opin Cell Biol* 31:46–55.
14. Del Valle-Pérez B, Arqués O, Vinyoles M, de Herreros AG, Duñach M (2011) Coordinated action of CK1 isoforms in canonical Wnt signaling. *Mol Cell Biol* 31:2877–2888.

15. Swiatek W, et al. (2004) Regulation of casein kinase I ε activity by Wnt signaling. *J Biol Chem* 279:13011–13017.
16. Cong F, Schweizer L, Varmus H (2004) Casein kinase Iepsilon modulates the signaling specificities of dishevelled. *Mol Cell Biol* 24:2000–2011.
17. Lee E, Salic A, Kirschner MW (2001) Physiological regulation of [β]-catenin stability by Tcf3 and CK1ε. *J Cell Biol* 154:983–993.
18. Hennings H, et al. (1983) Malignant conversion of mouse skin tumours is increased by tumour initiators and unaffected by tumour promoters. *Nature* 304:67–69.
19. Dotto GP, Parada LF, Weinberg RA (1985) Specific growth response of ras-transformed embryo fibroblasts to tumour promoters. *Nature* 318:472–475.
20. Parker PJ, et al. (1986) The complete primary structure of protein kinase C–The major phorbol ester receptor. *Science* 233:853–859.
21. Antal CE, et al. (2015) Cancer-associated protein kinase C mutations reveal kinase's role as tumor suppressor. *Cell* 160:489–502.
22. Mackay HJ, Twelves CJ (2007) Targeting the protein kinase C family: Are we there yet? *Nat Rev Cancer* 7:554–562.
23. Zhang LL, et al. (2015) The protein kinase C (PKC) inhibitors combined with chemotherapy in the treatment of advanced non-small cell lung cancer: Meta-analysis of randomized controlled trials. *Clin Transl Oncol* 17:371–377.
24. Stallings-Mann M, et al. (2006) A novel small-molecule inhibitor of protein kinase Ciota blocks transformed growth of non-small-cell lung cancer cells. *Cancer Res* 66:1767–1774.
25. Clark AS, West KA, Blumberg PM, Dennis PA (2003) Altered protein kinase C (PKC) isoforms in non-small cell lung cancer cells: PKCdelta promotes cellular survival and chemotherapeutic resistance. *Cancer Res* 63:780–786.
26. Valverde AM, Sinnett-Smith J, Van Lint J, Rozengurt E (1994) Molecular cloning and characterization of protein kinase D: A target for diacylglycerol and phorbol esters with a distinctive catalytic domain. *Proc Natl Acad Sci USA* 91:8572–8576.
27. Shindo M, et al. (2003) Synthesis and phorbol ester binding of the cysteine-rich domains of diacylglycerol kinase (DGK) isozymes. DGKgamma and DGKbeta are new targets of tumor-promoting phorbol esters. *J Biol Chem* 278:18448–18454.
28. Shindo M, Irie K, Ohigashi H, Kuriyama M, Saito N (2001) Diacylglycerol kinase γ is one of the specific receptors of tumor-promoting phorbol esters. *Biochem Biophys Res Commun* 289:451–456.
29. Ahmed S, et al. (1993) A novel functional target for tumor-promoting phorbol esters and lysophosphatidic acid. The p21rac-GTPase activating protein n-chimaerin. *J Biol Chem* 268:10709–10712.
30. Caloca MJ, Wang H, Kazanietz MG (2003) Characterization of the Rac-GAP (Rac-GTPase-activating protein) activity of β2-chimaerin, a 'non-protein kinase C' phorbol ester receptor. *Biochem J* 375:313–321.
31. Betz A, et al. (1998) Munc13-1 is a presynaptic phorbol ester receptor that enhances neurotransmitter release. *Neuron* 21:123–136.
32. Balmain A, Ramsden M, Bowden GT, Smith J (1984) Activation of the mouse cellular Harvey-ras gene in chemically induced benign skin papillomas. *Nature* 307:658–660.
33. Abel EL, Angel JM, Kiguchi K, DiGiovanni J (2009) Multi-stage chemical carcinogenesis in mouse skin: Fundamentals and applications. *Nat Protoc* 4:1350–1362.
34. Ise K, et al. (2000) Targeted deletion of the H-ras gene decreases tumor formation in mouse skin carcinogenesis. *Oncogene* 19:2951–2956.
35. Simanshu DK, Nissley DV, McCormick F (2017) RAS proteins and their regulators in human disease. *Cell* 170:17–33.
36. Shin I, Kim S, Song H, Kim HR, Moon A (2005) H-Ras-specific activation of Rac-MKK3/6-p38 pathway: Its critical role in invasion and migration of breast epithelial cells. *J Biol Chem* 280:14675–14683.
37. Wen-Sheng W (2006) Protein kinase C α trigger Ras and Raf-independent MEK/ERK activation for TPA-induced growth inhibition of human hepatoma cell HepG2. *Cancer Lett* 239:27–35.
38. Kundu JK, Shin YK, Surh YJ (2006) Resveratrol modulates phorbol ester-induced pro-inflammatory signal transduction pathways in mouse skin in vivo: NF-kappaB and AP-1 as prime targets. *Biochem Pharmacol* 72:1506–1515.
39. Li J, Ji L, Chen J, Zhang W, Ye Z (2015) Wnt/β-catenin signaling pathway in skin carcinogenesis and therapy. *BioMed Res Int* 2015:964842.
40. Gat U, DasGupta R, Degenstein L, Fuchs E (1998) De novo hair follicle morphogenesis and hair tumors in mice expressing a truncated β-catenin in skin. *Cell* 95:605–614.
41. Huelsken J, Vogel R, Erdmann B, Cotsarelis G, Birchmeier W (2001) β-catenin controls hair follicle morphogenesis and stem cell differentiation in the skin. *Cell* 105:533–545.
42. Malanchi I, et al. (2008) Cutaneous cancer stem cell maintenance is dependent on β-catenin signalling. *Nature* 452:650–653.
43. Schwarz M, Münzel PA, Braeuning A (2013) Non-melanoma skin cancer in mouse and man. *Arch Toxicol* 87:783–798.
44. Bhatia N, Spiegelman VS (2005) Activation of Wnt/β-catenin/Tcf signaling in mouse skin carcinogenesis. *Mol Carcinog* 42:213–221.
45. Lu D, Carson DA (2009) Spiperone enhances intracellular calcium level and inhibits the Wnt signaling pathway. *BMC Pharmacol* 9:13.
46. Červenka I, et al. (2011) Mitogen-activated protein kinases promote WNT/β-catenin signaling via phosphorylation of LRP6. *Mol Cell Biol* 31:179–189.
47. Bazzi H, Fantauzzo KA, Richardson GD, Jahoda CA, Christiano AM (2007) The Wnt inhibitor, Dickkopf 4, is induced by canonical Wnt signaling during ectodermal appendage morphogenesis. *Dev Biol* 305:498–507.
48. Davidson G, et al. (2005) Casein kinase 1 gamma couples Wnt receptor activation to cytoplasmic signal transduction. *Nature* 438:867–872.
49. Cruciat CM, et al. (2013) RNA helicase DDX3 is a regulatory subunit of casein kinase 1 in Wnt-β-catenin signaling. *Science* 339:1436–1441.
50. Kikkawa U, Takai Y, Tanaka Y, Miyake R, Nishizuka Y (1983) Protein kinase C as a possible receptor protein of tumor-promoting phorbol esters. *J Biol Chem* 258:11442–11445.
51. Kim S, Chun SY, Kwon YS, Nam KS (2016) Crosstalk between Wnt signaling and phorbol ester-mediated PKC signaling in MCF-7 human breast cancer cells. *Biomed Pharmacother* 77:114–119.
52. Gwak J, et al. (2009) Stimulation of protein kinase C-α suppresses colon cancer cell proliferation by down-regulation of β-catenin. *J Cell Mol Med* 13:2171–2180.
53. Lee H, Chen R, Lee Y, Yoo S, Lee C (2009) Essential roles of CKIdelta and CKIepsilon in the mammalian circadian clock. *Proc Natl Acad Sci USA* 106:21359–21364.
54. Schak KM, Harrington ME (1999) Protein kinase C inhibition and activation phase advances the hamster circadian clock. *Brain Res* 840:158–161.
55. Akashi M, Nishida E (2000) Involvement of the MAP kinase cascade in resetting of the mammalian circadian clock. *Genes Dev* 14:645–649.
56. Relles D, et al. (2013) Circadian gene expression and clinicopathologic correlates in pancreatic cancer. *J Gastrointest Surg* 17:443–450.
57. Rosenberg LH, et al. (2015) Therapeutic targeting of casein kinase 1δ in breast cancer. *Sci Transl Med* 7:318ra202.
58. Janovska P, et al. (2018) Casein kinase 1 is a therapeutic target in chronic lymphocytic leukemia. *Blood* 131:1206–1218.

CELL BIOLOGY